The Relationship between the Surface Composition and Electrical Properties of Corrosion Films Formed on Carbon Steel in Alkaline Sour Medium: An XPS and EIS Study

Policarpo Galicia, Nikola Batina, and Ignacio González*

Universidad Autónoma Metropolitana−Iztapalapa, Department of Chemistry, Area of Electrochemistry, Av. San Rafael Atlixco 186, col. Vicentina. 09340, México D.F., Mexico

Received: March 28, 2006; In Final Form: April 28, 2006

This work studies the evolution of 1018 carbon steel surfaces during 3−15 day immersion in alkaline sour medium 0.1 M $(NH_4)_2S$ and 10 ppm CN^- as (NaCN). During this period of time, surfaces were jointly characterized by electrochemical techniques in situ (electrochemical impedance spectroscopy, EIS) and spectroscopic techniques ex situ (X-ray photoelectron spectroscopy, XPS). The results obtained by these techniques allowed for a description of electrical and chemical properties of the films of corrosion products formed at the 1018 steel surface. There is an interconversion cycle of chemical species that form films of corrosion products whose conversion reactions favor two different types of diffusions inside the films: a chemical diffusion of iron cations and a typical diffusion of atomic hydrogen. These phenomena jointly control the passivity of the interface attacked by the corrosive medium.

1. Introduction

Alkaline sour medium is formed by a solution of $(NH_4)_2S$ and CN^-, and it is a common corrosive medium in catalytic oil plants. This solution mainly condenses in the extraction zones and naphtha/oil/light hydrocarbon containers, forming an interface between crude oil derivatives and the steel corroded by their presence. Most studies on steel corrosion in this medium carried out to date have been mainly performed by electrochemical techniques such as electrochemical impedance spectroscopy (EIS) and equivalent circuit models, and their results converge in the following corrosion mechanism:[1−7]

Adsorption of HS^- ions at the interface film−aqueous medium $HS^- \leftrightarrow HS^-_{ad}$ (1)

Reduction of HS^- ions $HS^-_{ad} + e^- \leftrightarrow H^0_{ad} + S^{2-}$ (2)

Formation of H_2 $2H^0_{ad} \leftrightarrow H_{2(g)}$ (3)

Iron oxidation $Fe^0 \leftrightarrow Fe^{2+}$ (4)

$Fe^{2+} \leftrightarrow Fe^{3+}$ (5)

Formation of nonstoichiometric iron sulfides and oxides

$xFe^{2+} + yS^{2-} \leftrightarrow Fe_xS_y$ (6)

$xFe^{2+} + yOH^- \leftrightarrow Fe_xO_y$ (7)

Diffusion of H^0 through the film

$H^0_{ad} \leftrightarrow H^0_{ab}$ (8)

where subindices ad and ab refer to the species adsorbed and absorbed onto iron, respectively, or to the film of corrosion products itself. Iron oxidation reactions (eqs 4 and 5) generate another diffusion process consisting of Fe cation displacement from the steel−film interface toward the film−solution interface due to the electrochemical potential. This displacement is characterized, in particular, by the change in the chemical environment experienced by the cation on its way through the films of corrosion products, because its coordination sphere and, in some cases, its oxidation status are modified, for which reason this process is often called chemical diffusion.[8]

The present model, however, does not contemplate in detail chemical species that participate in film formation and subsequent repercussions on their electrochemical behavior. This work was aimed to study the chemical composition of the films formed naturally (or by immersion) in sour medium 0.1 M $(NH_4)_2S$ and CN^- 10 ppm, during a period of 3−15 days. In this course of time, in situ characterizations of the forming films were made using electrochemical impedance spectroscopy (EIS), whereas ex situ characterizations were performed using X-ray photoelectron spectroscopy (XPS).

2. Experimental Methodology

2.1. Electrode Preparation. The first thing necessary in order to form corrosion films was to construct 1018 carbon steel disks of 8-mm radius and 1.5-mm thickness, which were then mounted on a Teflon cap leaving one side of the steel disk uncovered (active area) and the other provided with electric terminal. Then the active area was subjected to mechanical polishing with 600 grade silicon carbide paper. Finally, the electrode was rinsed with Millipore ultrapure water (18 MΩ).

2.2. Formation and Characterization of Corrosion Product Films by EIS. For film formation, a 45-mL vitreous cell with 5 inlets 0.1M $(NH_4)_2S$ was used as corrosive or growth solution prepared with the corresponding Aldrich AR salt, together with 10 ppm CN^- as NaCN of Merck AR brand. For this solution, Millipore ultrapure water (18 MΩ) previously deareated by bubbling N_2 was utilized. The immersion time of each steel electrode in the solution was 3, 5, 10, and 15 days. Upon completion of each period of immersion, $Hg/HgSO_{4(s)}/K_2SO_4$ (SSE) electrodes were incorporated into the cell with graphite

* To whom correspondence should be addressed. E-mail: qgalicia@yahoo.com.mx (P.G.), igm@xanum.uam.mx (I.G.) and bani@xanum.uam.mx (N.B.).

10.1021/jp061921k CCC: $33.50
Published on Web 07/01/2006

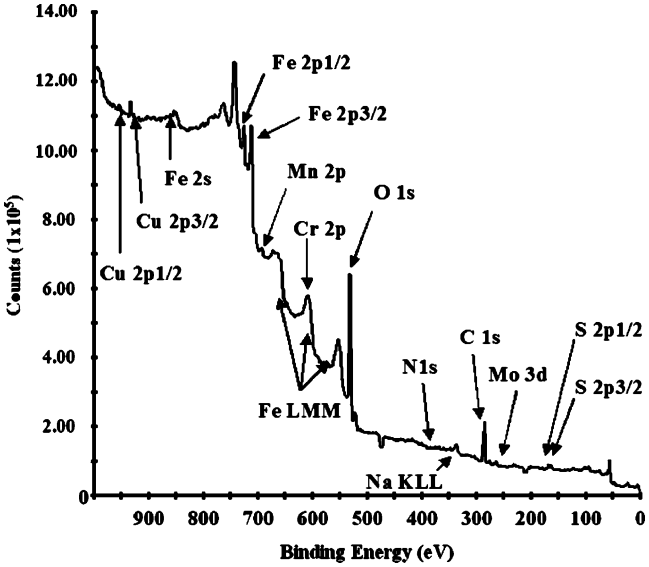

Figure 1. Representative XPS spectrum (Mg Kα) of the film deposited on the 1018 carbon steel during 15-day immersion in the medium 0.1 M $(NH_4)_2S$ and 10 ppm CN^-.

as counter-electrode to obtain corresponding impedance spectra using a potentiostat-galvanostat AUTOLAB PGSTAT30. The frequency scan was from 10 000 to 0.01 Hz at an amplitude of ±10 mV against corrosion potential. In previous works,[1,2] it has been shown that an amplitude of ±10 mV, for the EIS characterization of corrosion films formed into carbon steel/sour medium interface, follows the requirements of stabilty and linearity for Kramers−Kronig analysis.

2.3. Characterization of Corrosion Products by XPS. To diminish the effect of spontaneous oxidation of the film in atmosophere and water, first the electrode with the film, previously formed on carbon steel/sour medium, is cautiously removed from the electrochemical cell, and the Teflon cap and electric terminal of the steel electrode were removed, not touching the active side where the film was formed. A tiny jet of Millipore ultrapure water is left to fall over this side to remove the remains of the sour medium solution, which was immediately moved to a chamber with N_2 atmosphere (grade 6), and silica gel. The N_2 was constantly replaced, to diminish the presence of oxygen and water, for 2 days. After dehydration, the films are moved to the prechamber of XPS MICROLAB 350 equipment and left for another day in a vacuum; then, the samples are moved to the main chamber, and the pressure is left to diminish to 10^{-9} mbar to obtain spectra. A Mg (Kα) cathode with 15 kV voltage was used as an X-ray transmitter. The angle of incidence and separation of the cathode from the sample used in all experiments were 45° and 2.5 cm, respectively. With this strategy, we obtained reproducible results in two different experiments sets; in fact, the chemical compositions obtained with XPS are consistent with those previously reported for similar films.[9]

3. Results and Discussion

3.1. XPS Characterization of Corrosion Product Films from Sour Medium. To illustrate the methodology used in qualitative and quantitative XPS analyses of different films of corrosion products, the film formed for 15 days of immersion is analyzed in detail, but the same kind of analysis was performed with the other films. Figure 1 presents the complete XPS spectrum of the film formed during 15 days in the sour medium. It shows qualitatively the main elements that form typical corrosion products of this system and, besides, makes part of the alkaline sour medium solution: Fe (2p), O (1s), N (1s), C (1s), and S (2p). Other signals are also present, corresponding to elements such as: Mo, Mn, and Cu, from the alloy made up of 1018 steel and specimen holder (Cu), as well as another type of subsequent electronic relaxations resulting from X-ray bombing.

3.1.1. Deconvolution Modeling of the Main Film-Constituting Elements. Chemical species that form corrosion products were qualitatively analyzed using deconvolution or decomposition modeling of spectral signals of the main elements (Fe, O, N, C, and S) in characteristic spectra reported in the literature. Therefore, again, the film formed during 15 days and its corresponding spectra are used for illustration.

The assignment of spectral lines for Fe species and transition metals, in general, is complex due to the presence of regions of magnetic domain with different intensity and orientation, which gives rise to a Zeeman effect that broadens spectral lines. In addition, Fe may form a wide range of structures with O and S, causing a slight displacement of chemical field by broadening the spectral signals.[10,11] This phenomenon appears in the spectrum of the Fe 2p orbital (Figure 2a), for which reason it was decided to fit the spectrum at 5 different signals corresponding to 2 main signals of spin $^3/_2$, and 3 signals of spin $^1/_2$, which are satellites or mirror of those of spin $^3/_2$. The first main signal of spin $^3/_2$ at 710.98 eV (Figure 2a,i) contains an Fe^{2+}/Fe^{3+} mixture of the species FeO, FeS, $Fe(OH)_2$, $Fe(OH)_3$, FeOOH, Fe_2O_3, Fe_3O_4, $FeCO_3$, Fe−CO, and $FeSO_4$.[12−16,10,17−19] Likewise, the second signal of spin $^3/_2$ at 713 eV (Figure 2a,ii) comprises a mixture of the Fe^{2+}/Fe^{3+} species much richer in Fe^{3+} such as: FeOOH, Fe−OH, Fe−SO_4, in nonstoichiometric ratio and $Fe_2(SO_4)_3{\cdot}7H_2O$.[13,18] The satellite signal of spin $^1/_2$ at 724.1 eV (Figure 2a,iii) confirms the presence of Fe_2O_3, Fe_3O_4, FeOOH, $FeCO_3$, Fe−CO, and FeS,[12,15−18] whereas the second satellite at 725.77 eV (Figure 2a,iv) confirms the presence of iron sulfates of nonstoichiometric nature.[12,17,18] Finally, the satellite signal corresponding to 717.66 eV (Figure 2a,v) confirms the presence of nonstoichiometric species FeOOH and Fe_2O_3.[17,20,21]

Figure 2b shows the partial spectrum of oxygen 1s where three characteristic signals, corresponding to O^{2-} at 530.01 eV (Figure 2b,i) from FeO, FeOOH, Fe_2O_3 and Fe_3O_4 are observed.[12,14,18,22] At 531.49 eV, the presence of OH^- (Figure 2b,ii) corresponding to nonstoichiometric FeOOH, $Fe(OH)_3$, and Fe−OH becomes visible.[12,15,17,18,21,22] Finally, adsorbed species $O^{(-)}$, OH^-, and H_2O are observed at 532.55 eV (Figure 2b,iii),[12,14,22,23] as well as SO_4^{2-} and CO^-[13,14,17,18,24] from solid species. This spectrum confirms the presence of most oxides and hydroxides suggested in the iron spectrum, but these are nonstoichiometric species, and the presence of $Fe(OH)_2$ is discarded because of its character of unstable intermediary in a highly corrosive medium as the alkaline sour medium.

The N 1s spectrum exhibits the smallest emission of photoelectrons. It is fundamentally the matter of the presence of CN^- and NH_3 at 399.5 eV (Figure 2c,i),[13,15,23] with small traces of ammonium salts at 401 eV (Figure 2c,ii).[13,23,24]

The deconvolution of the carbon 1s is also composed of three different signals: C−H at 284.66 eV (Figure 2d,i),[13,14,17,25] and it is a product of contamination after manipulating already formed CO^- films from solid nonstoichiometric species at 285.9 eV (Figure 2d,ii),[13,25] whereas at 288.08 eV (Figure 2d,iii), $FeCO_3$ and CO_2 appear,[17,15] together with traces of CN^-.[13]

In the partial spectrum of S 2p (Figure 2e), there are two different signals corresponding to S^{2-} and S^{6+} species at 163

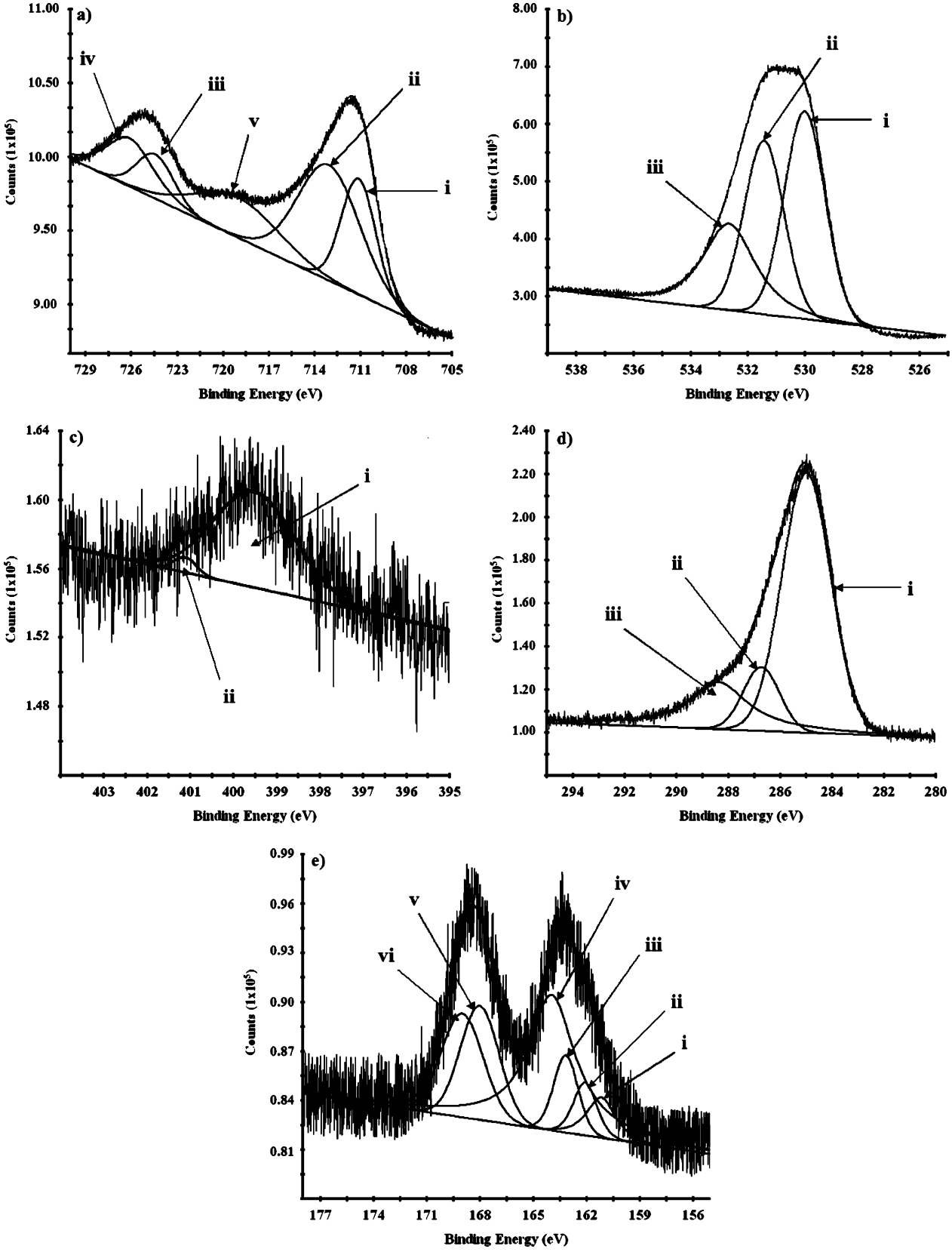

Figure 2. Spectroscopic characterization of the film deposited on the 1018 carbon steel during 15-day immersion in the medium 0.1 M $(NH_4)_2S$ and 10 ppm CN^-. Representative XPS spectra of the (a) iron 2p region, (b) oxygen 1s, (c) nitrogen 1s, (d) carbon 1s, and (e) sulfur 2p region. Each spectrum shows the principal signals used in its fitting.

and 168.5 eV, respectively, which themselves are composed of a mixture of spin $^3/_2$ and $^1/_2$ orbitals each. The deconvolution that fits best to the signal of 163 eV comprises four different signals. The first main signal of spin $^3/_2$ at 161.16 eV (Figure 2e,i) corresponds to FeS and $Fe_{1-x}S$.[26−28,15,13] The second, again of spin $^3/_2$, at 162.06 eV (Figure 2e,ii) corresponds to −S−S− dimer of FeS_2 together with Fe polysulfides (Fe_xS_y).[11,15,26,27] The third at 163.15 eV (Figure 2e,iii) comprises a mixture of signals

TABLE 1: Variation of Elementary Atomic Percentage of the Main Elements Forming 1018 Carbon Steel Corrosion Products as a Function of Time of Immersion in the Medium 0.1 M $(NH_4)_2S$ and 10 ppm CN^-[a]

alkaline sour medium	element	Time in days (atomic percent) 3	5	10	15
0.1 M	O	47.5	46.8	49.0	44.3
	Fe	29.4	32.6	30.4	42.3
	C	20.4	18.4	17.7	11.9
	N	1.4	0.5	1.1	0.4
	S	1.3	1.7	1.8	1.1
1 M	N	1.3	1.1	1.0	1.2
	S	2.2	3.1	2.0	4.0

[a] In the case of Fe and S, only the signals of spin $^3/_2$ corresponding to deconvolution modeling were taken into account.

of spin $^3/_2$ and $^1/_2$, corresponding to S_8 and satellite signals of FeS and FeS_2.[11,15,26,28] Finally, the signal at 163.96 eV (Figure 2e,iv) comprises just one signal of spin 1/2, corresponding to satellite signals of S_8 and Fe_xS_y of Fe.[29−31] The signal corresponding to S^{6+} at 168.5 eV is composed of only two signals, the main one grouping together the SO_4^{2-} at 168.01 eV (Figure 2e,v), and its satellite at 168.99 eV (Figure 2e,vi), thus confirming the presence of nonstoichiometric Fe−SO_4[13,26,27,29,32] generated by iron sulfide oxidation.

3.1.2. Elementary Composition of the Films as a Function of Immersion Time. Results of the elementary XPS analysis of the films formed by immersion into sour medium are shown in Table 1. Fe and S films were calculated based on deconvolution modeling, considering only spin $^3/_2$ orbitals, but not the satellite signals. The films observed are mainly formed by O, with an initial composition of 47.5% at 3 days of immersion that slightly decreases to 44.3% by the day 15. In the second place of importance is Fe, whose concentration increases form 29.4−42.3% within the same time of immersion, indicating the continuation of steel dissolution despite the existence of a film which isolates it from the corrosive medium. It is proper to mention that trends observed for these elements are inverted in the film corresponding to 10 days of immersion. The concentration of carbon, which occupies the third place in terms of concentration, decreases from 20.4 to 11.9% as the time of immersion and consequent film formation increases.

The concentration of N and S, however, varies within the range of 1.4−0.4% and 1.8−1.1%, respectively, being lower than expected, especially for sulfur. Therefore, it was decided to repeat XPS experiments for these elements, but on the films formed in a 10-fold more concentrated solution of 1 M $(NH_4)_2S$. The maximum amount of N found in these new films was scarcely 1.3% after 3 days of immersion, which demonstrates the lack of importance of this element among corrosion products because, according to spectrum deconvolution (Figure 2c), only CN^- and NH_3 are contained in the film. S concentration, however, reaches its maximum of 4% at 15 days of damaging, but due to the great variety of species it forms, its analysis is deemed necessary.

3.1.3. Distribution of Chemical Species Constituting Films Formed during Different Times of Immersion. The distribution of chemical species determined by spectral deconvolution of the films formed onto 1018 carbon steel during different times of immersion in alkaline sour medium are shown in Table 2. The analysis was carried out similarly to that described in the previous section taking into consideration again the main signals of spin $^3/_2$ for Fe and S. As can be observed for the three groups of species assigned for O, there are small variations of concentration throughout the time of damaging. The main group

TABLE 2: Distribution of Different Chemical Species Determined by Deconvolution of Partial XPS Spectra of the Films Formed on 1018 Carbon Steel as a Function of Different Times of Immersion in the Medium 0.1 M $(NH_4)_2S$ and 10 ppm CN^-[a]

element	chemical species	Atomic percent (time in days) 3	5	10	15
oxygen	FeO, FeOOH, Fe_2O_3, Fe_3O_4	37.67	35,46	38.52	41.13
	FeOOH, Fe(OH), Fe-OH	31.09	36,10	30.88	33.55
	$O^{(-)}_{ad}$, OH_{ad}, H_2O_{ad}, SO_4^{2-}, CO^-	31.24	28,44	30.60	25.32
carbon	C-H	57.27	67.87	60.77	64.52
	CO^-	24.31	14.21	23.92	11.27
	$FeCO_3$, CO_2, CN^-	18.42	17.91	15.31	24.21
nitrogen	CN^-, NH_3	100.00	100.00	64.30	95.91
	NH_4^+	0.00	0.00	34.70	4.09
sulfur	FeS, $FE_{1-x}S$	12.51	15.55	0.00	14.44
	FeS_2, Fe_xS_y	14.73	7.11	11.31	14.37
	S_8, $FeS_{2,sat}$	24.32	14.51	8.93	21.49
	SO_4^{2-}	49.00	62.84	79.76	49.69

[a] In the case of Fe and S, only the signals of spin $^3/_2$ corresponding to deconvolution modeling were taken into account.

corresponds to that formed by oxides: FeO, FeOOH, Fe_2O_3, and Fe_3O_4 that increase their concentration as of 5 days of immersion until reaching a maximum of 41% at 15 days of immersion. This proves that the film itself experiences oxidation and/or dehydration of simple species such as hydroxides as well as of adsorbed species whose decomposition probably generates H^0. The second important appearance is that of hydroxides: nonstoichiometric FeOOH, $Fe(OH)_3$, and Fe−OH that serve as intermediaries in the formation of oxides and whose concentration varies inversely to that of oxides in the range of 30.9−36.1% (10 and 5 days, respectively). The SO_4^{2-} and CO^-, together with the adsorbed species $O^{(-)}$, OH^-, and H_2O, represent the smallest amount of oxygen present in the films with a concentration that decreases from 31.2% after 3 days of formation to 25.3% at 15 days, thus confirming the inverse behavior from that observed in oxides.

The C present in the films of corrosion products is found for the most part as impurity (C−H), followed by the nonstoichiometric species of CO^- that decrease as the time of immersion increases from 24.3 to 11.3%, surely due to reduction in gases entrapped in the film-forming cell. Likewise, the same behavior is observed in the species of $FeCO_3$, CO_2, and CN^- (18.4−5.3%); however, the trend is again interrupted at 15 days of immersion.

In the case of nitrogen, the presence of ammonium salts was detected at immersion times above 10 days; it appears mostly as NH_3, because the concentration of CN^- in the solution is very small (10 ppm).

Finally, the S present in the form of different iron sulfides varies irregularly for these species due to the low concentration of these sulfides (FeS 12.51% and FeS_2 7.11%). In this manner, the signal corresponding to S_8 and satellite signals of the different sulfides (Figure 2b,iii) suggest that the presence of S_8 must be minimum. In contrast, the SO_4^{2-} represents the greatest amount of S, with a maximum 50.6% reached at 10 days of immersion. This behavior is consistent with references from the literature where different iron sulfides are mentioned to be easily oxidized to sulfates and intermediaries such as S_8, little stable in corrosive media and O_2.[26,27,29,32]

3.2. Electrochemical Impedance Spectra Analysis of the Films Formed during Different Times of Immersion in the Sour Medium. Figure 3 shows the electrochemical impedance

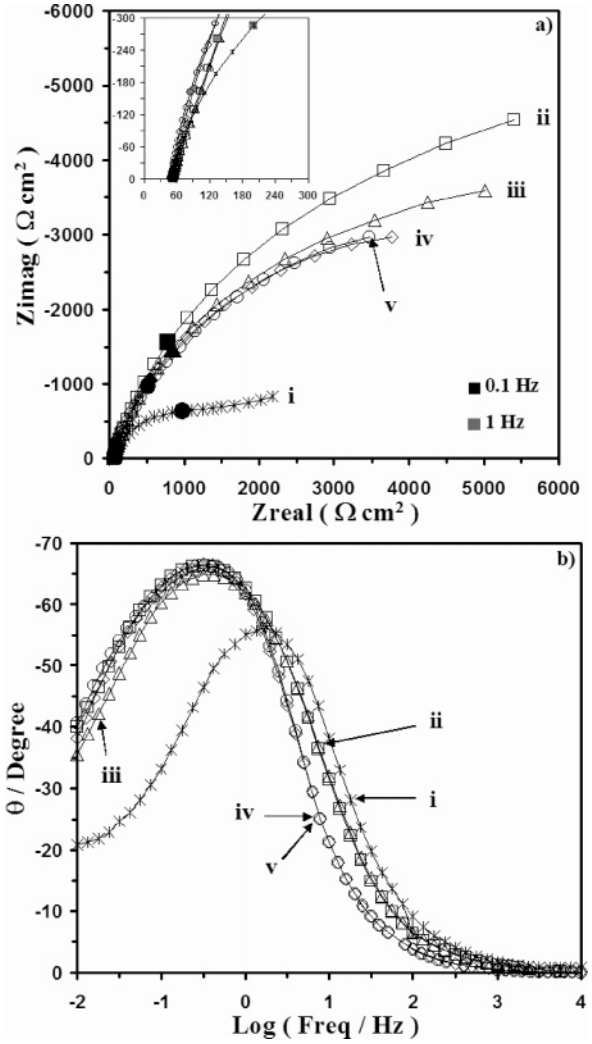

Figure 3. (a) Nyquist complex diagram and (b) Bode phase angle diagram of the corrosion product films naturally formed on the 1018 carbon steel during (i) 0, (ii) 3, (iii) 5, (iv) 10, and (v) 15 days of immersion in the medium 0.1 M $(NH_4)_2S$ and 10 ppm CN^-.

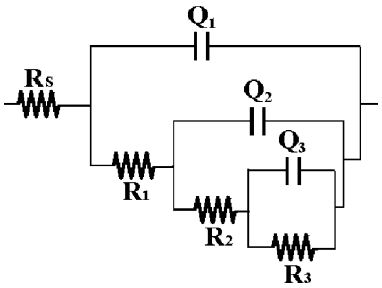

Figure 4. Equivalent circuit used to describe EIS spectra of the films deposited on the 1018 carbon steel by different times of immersion in the medium 0.1 M $(NH_4)_2S$ and 10 ppm CN^-. This model considers steel oxidation (R_1) double-layer capacitance (Q_1) and diffusion processes of iron and atomic hydrogen cations through the films of corrosion products (R_2-Q_2 and R_3-Q_3, respectively).

spectra corresponding to the films formed at different immersion times during which the 1018 steel was exposed to the sour medium.

The quantitative analysis of these spectra was performed using the equivalent circuit shown in Figure 4, which has been previously used in the evaluation of the corrosion mechanism in the sour medium.[1−4] A detailed analysis of time-constant identification of these diagrams has been previously reported.[33] In this model, the solution resistance is represented by the electric component R_s. Charge-transfer resistance, R_1, describes the extent to which the formation of iron cations is favored at the steel−film interface. The constant phase element, Q_1, allows for calculating the nonideal capacitance of the electrochemical double layer (C_{HF}) and treats the film of corrosion products as a dielectric using the following equation.[1−4]

$$C_{HF} = (Y_0 R_{HF})^{1/n}/R_{HF} \quad (9)$$

where Y_0 is the base admittance of the constant phase element Q_1, R_{HF} is the resistance at high frequencies R_1, and n is a factor that satisfies the condition $0 \le n \le 1$, which indicates how far (0), or how close (1), the interface is from being treated as an ideal capacitor.

On the other hand, parallel arrays $\mathbf{R_2-Q_2}$ and $\mathbf{R_3-Q_3}$ describe diffusion processes of iron cations and atomic hydrogen, respectively, through the film of corrosion products. Iron diffusion is not a question of cation displacement but of chemical diffusion in which the chemical environment of the cation is being modified as it displaces from the steel−film interface toward solution. The hydrogen atomic diffusion inside of corrosion films formed in the interface carbon steel/sour medium is a commonly phenomenon associated to this kind of chemical environment, provoking blister corrosion; however, the electrochemical study of this phenomenon is still controversial. In a previous papers,[33,34] experimental proofs were presented to demonstrate the existence of the atomic hydrogen diffusion through the films; furthermore, in this paper, this phenomenon has been associated with the electrical array $\mathbf{R_3-Q_3}$ used in the corresponding EIS experimetal analysis. This strategy has been used to describe the corrosion process of carbon steel in sour media.[1−4,7,8,33,34]

Altogether, both phenomena, diffusion of iron cations and atomic hydrogen through the film of corrosion products, are the first in being responsible for the current phase shift that chemically and physically depends on the type of corrosion product obtained.

3.2.1. High-Frequency Analyses. The values of electric elements obtained from the best fits of EIS spectra for the films corresponding to different times of immersion are summarized in Table 3. The R_s varies within the range of 48−52 Ω, suggesting that the film growth medium remains constant during different times of steel immersion. The value of resistance to transfer charge (R_1) decreases from 64 Ω cm² in the clean steel up to 12 Ω cm² for the films formed during 3 and 5 days, thereby favoring anodic dissolution of iron for these films. At longer immersion times, the dissolution becomes slower, as shown by the values of 47 and 46 Ω cm² for the films formed during 10 and 15 days, respectively. The values of n_1 increase from 0.81 in the steel recently immersed to 0.91 in the film formed during 15 days, suggesting the formation of physically more homogeneous films at longer times of immersion in the sour medium. These values of n allow for making a precise calculation of the capacitance with eq 9. The value obtained for the film formed instantaneously on the steel recently immersed (268 μf) is slightly greater than that observed in the films formed at times below 5 days, suggesting that the initial film is composed of adsorbed species such as HS^-, CO_2, OH^-, and H_2O, that even before initiating the iron oxidation reaction forms a layer that gets more compact with the progress of oxidation in different iron precipitates. For already formed films, the capacitance increases progressively from 183 μf in the 3-day film to 622 μf at 15 days. This indicates that the thickness of the films increases and their chemical composition is modified,

TABLE 3: Values of Electric Components Obtained from the Best Fit with the Equivalent Circuit from Figure 4, EIS Diagrams of the Films Formed on 1018 Carbon Steel, During Different Times of Immersion in the Medium 0.1 M $(NH_4)_2S$ and 10 ppm CN^-

		Q_1				Q_2			Q_3		
time in days	R_s (Ω)	R_1 (Ω)	$Y_{01} \times 10^{-4}$ (mho·s^n)	$n1$	C_{HF} (μf)	R_2 (Ω)	$Y_{02} \times 10^{-4}$ (mho·s^n)	$n2$	R_3 (Ω)	$Y_{03} \times 10^{-4}$ (mho·s^n)	$n3$
0	50	64	5.8	0.81	268	1300	0.4	1	1800	3.3	0.68
3	52	12	5.57	0.82	183	9910	2.42	0.82	4000	52.3	0.97
5	52	12	6.03	0.81	192	7640	1.91	0.84	2930	53.5	0.95
10	51	47	9.34	0.87	586	2200	1.56	1	6850	5.71	0.66
15	48	46	8.56	0.91	622	1250	2.07	1	8110	6.38	0.64

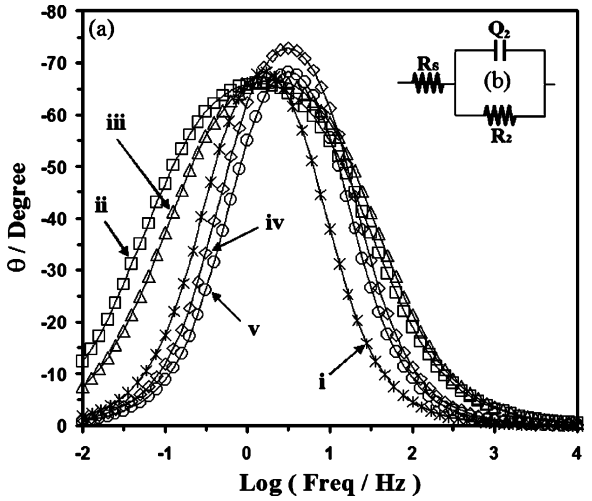

Figure 5. (a) Analysis of the frequency range with manifestations of iron cation diffusion through the films of corrosion products during (i) 0, (ii) 3, (iii) 5, (iv) 10, and (v) 15 days of immersion in the medium 0.1 M $(NH_4)_2S$ and 10 ppm CN^-. (b) Equivalent circuit used in the construction of phase shift angle diagram with electric elements of Table 3.

as shown in the XPS analysis, together with their rugosity (see *n* values in Table 3).

3.2.2. Analysis of Iron and Atomic Hydrogen Diffusion Processes. In the parallel array $\mathbf{R_2}-\mathbf{Q_2}$ that describes chemical diffusion of iron cations through the film, R_2 and Y_{02} values of the formed films are higher than in the steel recently immersed (Table 3), because of the increased thickness of the films resulting from a longer time of immersion. These electric components reach their maximum value in a 3-day film and from then on, they progressively decrease (except for Y_{02} in the 15-day film), which proves that iron diffusion is favored by increased time of steel immersion into the sour medium. On the basis of the data of Table 3, Figure 5 represents the phase angle diagram in relation to frequency for the circuit R_s in series with the array $\mathbf{R_2}-\mathbf{Q_2}$. The comparison of this diagram with the corresponding experimental diagrams (Figure 3b) allows evaluating the frequency range within which this time constant is manifested in the overall behavior of EIS spectrum (Figure 3b). Thus, it is observed that iron diffusion in the 3-day film (Figure 5 i) spanning about four frequency decades, from 100 to 0.01 Hz. This range of frequencies decreases progressively until spanning 2 decades in the 15-day film (Figure 5 v). Moreover, there is a slight shift in high frequencies and another, more intense in low frequencies of approximately one decade, suggesting that the diffusion is relatively more rapid and, consequently, more favored at longer times of immersion.

Such behavior is corroborated by the increase in the concentration of Fe cations from the elementary analysis (Table 1), and the distribution of species from XPS (Table 2). They show that the trend exhibited by oxides is contrary to that of hydroxides and similar to that of adsorbed species (except for 10-day immersion), suggesting the presence of conversion of species: adsorbed oxygen is transformed into hydroxides, which themselves are transformed into oxides as shown by the following equations:[17,35−38]

$$Fe^{2+} + 2OH^- \leftrightarrow Fe(OH)_2 \quad (10)$$

$$Fe(OH)_2 + OH^- \leftrightarrow Fe(OH)_3 \quad (11)$$

$$2Fe(OH)_2 \leftrightarrow 2FeOOH + H_2 \quad (12)$$

$$Fe(OH)_2 \leftrightarrow FeO + H_2O \quad (13)$$

$$4FeO + 2H_2O \leftrightarrow 2Fe_2O_3 + 2H_2 \quad (14)$$

$$3FeO + H_2O \leftrightarrow Fe_3O_4 + H_2 \quad (15)$$

$$4Fe_3O_4 + 2H_2O \leftrightarrow 6Fe_2O_3 + 2H_2 \quad (16)$$

$$2Fe_3O_4 + 4H_2O \leftrightarrow 6FeOOH + H_2 \quad (17)$$

It means that the iron indeed favors its chemical diffusion, as shown by the chemical evolution of the oxides. Moreover, these oxides may also be transformed into other species due to the presence of CO_2,[17,36] which additionally promotes iron diffusion.

$$3FeO + CO_2 \leftrightarrow Fe_3O_4 + CO \quad (18)$$

$$FeCO_3 + 2FeO \leftrightarrow Fe_3O_4 + CO \quad (19)$$

$$FeO + CO_2 \leftrightarrow FeCO_3 \quad (20)$$

This conversion of species also takes place with sulfur, because different iron sulfides may relatively easily be oxidized to sulfates by a gradual and repetitive degradation, through intermediaries such as S_8 and other intermediaries unstable in this medium, such as $S_2O_3^{2-}$ and SO_3^{2-}.[26,30,35,39,40]

$$2Fe_{1-x}S + yO_2 + 2yH_2O \leftrightarrow 2yFe^{2+} + 4yOH^- + 2Fe_{1-x-y}S \quad (21)$$

$$FeS_2 + 7/2O_2 + 2OH^- \leftrightarrow Fe^{2+} + 2SO_4^{2-} + H_2O \quad (22)$$

$$8S_2O_3^{2-} \leftrightarrow S_8 + 8SO_3^{2-} \quad (23)$$

$$2SO_3^{2-} + O_2 \leftrightarrow 2SO_4^{2-} \quad (24)$$

$$Fe^{2+} + SO_4^{2-} \leftrightarrow FeSO_4 \quad (25)$$

Atomic hydrogen diffusion (R3 Q3), however, depends directly on the species that generate it, such as HS^-, $O^{(-)}$, H_2O, HO^-, and iron hydroxides. Due to small amounts of sulfur found in the films (Table 1), it is possible to assume that hydrogen generation depends almost completely on oxygen compounds determined by XPS. The frequency range within which H^0

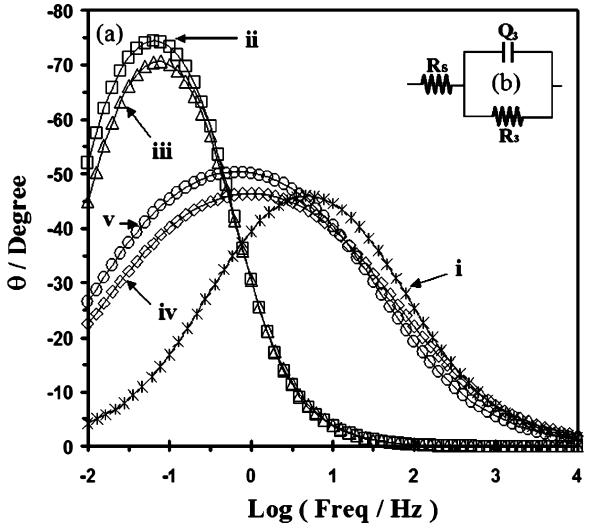

Figure 6. (a) Analysis of the frequency range with manifestations of H0 diffusion through the films of corrosion products during (i) 0, (ii) 3, (iii) 5, (iv) 10, and (v) 15 days of immersion in the medium 0.1 M $(NH_4)_2S$ and 10 ppm CN^-. (b) Equivalent circuit used in the construction of diagrama phase shift angle diagram with electric elements of Table 3.

diffusion is manifested is again graphically illustrated by circuit angle diagram: R_s in series with the array $\mathbf{R_3-Q_3}$, construted with the corresponding values of Table 3 (Figure 6). For the steel at the initial immersion time, this phenomenon spans a little bit more than three frequency decades (Figure 6 i), appearing at about 10 Hz and occurring more rapidly than that observed in a typical hydrogen diffusion (0.1−0.01 Hz).[1−4,33] This is because of a primary film formed on the steel in contact with the sour medium, which is mainly made up of adsorbed species (HS^-, $O^{(-)}$, CO_2, H_2O, HO^-) and gel-like iron precipitates that favor absorption of species and makes H^0 diffusion overlap with the diffusion of iron species (Figure 3b). The behavior exhibited by the films formed during 3 and 5 days (Figure 6 ii and iii) is a typical H^0 diffusion.[1−4] It is slightly favored by larger time of immersion because of increased H_2 concentration resulting from the conversion of species (eqs 12, 14−17) with the implicit involvement of H^0 (eq 3). However, at immersion times above 10 days (Figure 6 iv and v), the behavior exhibited is similar to that of steel recently immersed (Figure 6 i), though slower, as shown by one-decade displacement toward lower frequencies compared to steel recently immersed, and manifested within a broader range of frequencies (more than four decades). Such behavior suggests that at longer times of immersion, surface homogeneity of the film interferes with H^0 diffusion (see *n* values in Table 3). At the same time, there is an increase in iron concentration and a decrease in oxygen that give rise to the insertion of iron cations into the oxides such as Fe_3O_4 and Fe_2O_3, (Table 2) forming oxygen-poor iron oxides with no formation of H^0. Despite this fact, the hydrogen diffusion in these films (Figure 6 iv, v) is faster than that in the films formed for 3 and 5 days (Figure 6 ii, iii); this could indicate the modification of the film structure due to the higher iron species released in the steel−film interface.

4. Conclusions

The XPS analysis determined that the films formed on the 1018 carbon steel using different times of immersion (3−15 days) in alkaline sour medium are mainly composed of oxygen in the form of oxides and carbonates and, to a much lower extent, of sulfur, in the form of sulfides and sulfates. Electrochemical behavior of these films (electrochemical impedance) depends directly on the chemical species they are made of, because as determined in this study the conversion of chemical species from adsorbed species to oxides, carbonates and sulfates (more stable in this medium) additionally promotes chemical diffusion of iron cations from the steel−film interface toward the film−solution interface. This same conversion of species promotes the formation of H_2 (eqs 2, 12, and 14−17) that implicitly generates a greater amount of H^0 (eq 3), thus increasing the chemical potential that favors its diffusion. However, at immersion times above 10 days, this phenomenon loses intensity due to formation of a superficially more homogeneous film and a decrease in dehydration reactions involving hydrogen; however, modification of the film structure due to the higher iron species released in the steel−film interface, the hydrogen diffusion in these films is faster.

Acknowledgment. P.G. is grateful to CONACyT for his postgraduate fellowship. We are also grateful for the financial aid of CONACyT, project SEP-2004-C01-47162 and IMP, project FIES-98-100-I.

References and Notes

(1) Cabrera-Sierra, R.; García, I.; Sosa, E.; Oropeza, T.; González, I. *Electrochim. Acta* **2000**, *46*, 487−497.
(2) Sosa, E.; Cabrera-Sierra, R.; Marina Rincon, E.; Oropeza, M. T.; González, I. *Electrochim. Acta* **2002**, *47*, 1197−1208.
(3) Sosa, E.; Cabrera-Sierra, R.; García, I.; Sosa, E.; Oropeza, M. T.; González, I. *Corros. Sci.* **2002**, *44*, 1515−1528.
(4) Cabrera-Sierra, R.; Miranda-Hernández, M.; Sosa, E.; Oropeza, T.; González, I. *Corros. Sci.* **2001**, *43*, 2305−2324.
(5) Wilhem, S. M.; Abayarathna, D. *Corrosion* **1994**, *50*, 152.
(6) Vera, J.; Kapusta, S.; Hackerman, N. *J. Electrochem. Soc.* **1986**, *133*, 461.
(7) Egorov, V. V.; Batrakov, V. V. *Russ. J. Electrochem.* **2000**, *36*, 1293.
(8) Sosa, E.; Cabrera-Sierra, R.; Oropeza, M. T.; Hernández, F.; Casillas, N.; Tremont, R.; Cabrera, C.; González, I. *Electrochim. Acta* **2003**, *48*, 1665−1674.
(9) Sosa, E.; Cabrera-Sierra, R.; Oropeza, M. T.; Hernández, F.; Casillas, N.; Tremont, R.; Cabrera, C.; González, I. *J. Electrochem. Soc.* **2003**, *150*, 530−535.
(10) Weissenrieder, J.; Göthelid, M.; Mansson, M. *Surf. Sci.* **2003**, *527*, 163−172.
(11) Nesbitt, H. W.; Scaini, M.; Höchst, H. *Am. Mineral.* **2000**, *85*, 850−857.
(12) Grosvenor, A. P.; Kobe, B. A.; McIntyre, N. S. *Surf. Sci.* **2004**, *572*, 217−227.
(13) Sastri, V. S.; Elboujdaini, M.; Brown, J. R. *Corros. Sci.* **1996**, *52*, 447−452.
(14) Olefjord, I.; Brox, B.; Jelvestam. U. *Sci. Technol.* **1985**, *133*, 2854−2861.
(15) http://srdata.nist.gov/xps.
(16) Roosendaal, S. J.; Van Asselen, B.; Elsenaar, J. W. *Surf. Sci.* **1999**, *442*, 329−337.
(17) Heuer, J. K.; Stubbins, J. F. *Corros. Sci.* **1999**, *41*, 1231.
(18) Brion, D. *Appl. Surf. Sci.* **1980**, *5*, 133−152.
(19) Rath, R. K.; Subramanian, S.; Pradeep, T. *J. Colloid Interface Sci.* **2000**, *229*, 82−91.
(20) Ishida, M.; Akao, N.; Hara, N. Corrosion and Electrochemical Characteristics of NiO−Cr2O3−F2O3 Artificial Passivation Films Formed By MOCVD. *Electrochemical Society Proceeding*, **1999**, *99−42*, 305−312.
(21) Oszkó, A.; Kiss, J.; Kiricsi, I. *Phys. Chem. Chem. Phys.* **1999**, *1*, 2565−2568.
(22) Mayer, Th. *Appl. Surf. Sci.* **2001**, *179*, 257−262.
(23) Li, P.; Lin, J. Y.; Tan, L. *Electrochim. Acta* **1997**, *42*, 605−615.
(24) Ochoa, N.; Baril, G.; Moran. F. *J. Appl. Electrochem.* **2002**, *32*, 497−504.
(25) Smith, K. L.; Hammond, J. S. *Appl. Surf. Sci.* **1985**, *22−23*, 288−298.
(26) Parker, A.; Klauber, C.; Kougianos, A. *Hydrometallurgy* **2003**, *71*, 265.
(27) Buckley, A. N. *Appl. Surf. Sci.* **1985**, *20*, 472−480.
(28) Leiro, J. A.; Mattila, S. *Surf. Sci.* **2003**, *547*, 157−161.
(29) Panzner, G.; Egert, B. *Surf. Sci.* **1984**, *144*, 651−664.

(30) Buckley, A. N. *Appl. Surf. Sci.* **1987**, *27*, 437−452.
(31) Velásquez, P.; Ramos-Barrado, J. R.; Cordova, R. *Surf. Interface Anal.* **2000**, *30*, 149−153.
(32) Godočíková, E.; Baláž P.; Bastl, Z. *Appl. Surf. Sci.* **2002**, *200*, 36−47.
(33) Galicia, P.; González, I. *Electrochim. Acta* **2005**, *50*, 4451.
(34) Cabrera-Sierra, R.; Sosa, E.; Oropeza, M. T.; González, I. *Electrochim. Acta* **2002**, *47*, 2149.
(35) Magnacca, G.; Cerrato, G.; Morterra, C.; Signoretto, M. *Chem Mater.* **2003**, *15*, 675−687.
(36) Vikesland, P. J.; Valentine, R. L. *Environ. Sci. Technol.* **2002**, *36*, 512.
(37) Musié, S.; Nowik, I.; Ristié, M.; Orehovec, Z. *Croat. Chem Acta* **2004**, *77*, 141−151.
(38) Kim, D. K.; Mikhaylova, M.; Zhang, Y.; Muhammed, M. *Chem. Mater.* **2003**, *15*, 1617−1627.
(39) Zhang, X.; Borda, M. J.; Schoonen, M. A. A.; Strongin, D. R. *Langmuir* **2003**, *19*, 8787−8792.
(40) Usher, C. R.; Cleveland, C. A.; Strongin, D. R.; Schoonen, M. *Environ. Sci. Technol.* **2004**, *38*, 5604−5606.